INTERNATIONAL JOURNAL FOR NUMERICAL METHODS IN FLUIDS, VOL. 9, 1381–1394 (1989)

# A NUMERICAL STUDY OF HEAT AND MOMENTUM TRANSFER FOR TUBE BUNDLES IN CROSSFLOW

YEON CHANG*, ANTONY N. BERIS† AND EFSTATHIOS E. MICHAELIDES*

*Department of Mechanical Engineering, †Department of Chemical Engineering, University of Delaware, Newark, DE 19716, U.S.A.

## SUMMARY

A numerical scheme is developed to predict the heat transfer and pressure drop coefficients in flow through rigid tube bundles. The scheme uses the Galerkin finite element technique. The conservation equations for laminar steady-state flow are cast in the form of streamfunction and vorticity equations. A Picard iteration method is used for the solution of the resulting system of non-linear algebraic equations. Results for the heat transfer and pressure drop coefficients are obtained for tube arrays of pitch ratios of 1·5 and 2·0. Very good agreement of the present results and experimental data obtained in the past is observed up to Reynolds numbers of 1000. It is also observed that the results of the present method show better agreement with the experimental data and that they are applicable for higher Reynolds numbers than results of other studies.

KEY WORDS Heat exchangers Crossflow Tube bundle Nusselt number Streamfunction/vorticity

## 1. INTRODUCTION

Tubular heat exchangers are found in many energy conversion and chemical reaction systems ranging from nuclear reactors to refinery condensers. The most important design variables of the tubular heat exchangers are the outside heat transfer coefficient of the tubes and the pressure drop of the fluid flowing externally (shell side pressure drop).

Correlations of experimental data were used in the past for the determination of the heat and momentum transfer in tube bundles. Some of the earlier studies of Grimison,[1] Bergelin *et al.*[2,3] and Gram *et al.*[4] provided the experimental data on which correlations were based. The use of correlations for design purposes often involved extrapolation of data beyond their region of validity, thus resulting in significant errors. This fact triggered the appearance of semi-analytical approaches to the problem of heat and momentum transfer, which together with the experimental studies provided a more reliable method for design. An outline of these studies may be found in a review article by Zukauskas[5] and in two books by Mueller[6] and Zukauskas and Ziugzda.[7]

The rapid development of computers has recently resulted in the use of numerical simulations for the solution of heat and momentum transfer problems in tubular heat exchangers. Ishihara and Bell[8] obtained the friction coefficients of tube bundles up to Reynolds numbers of 100. Le Feuvre[9] and also Launder and Massey[10] obtained results in the laminar and turbulent regions for two cylinders in a row, and Fujii *et al.*[11] extended the calculations in the laminar region for five cylinders. Antonopoulos[12] first made calculations in the laminar regime and later[13] used a numerical scheme to predict the flow characteristics in straight and inclined tube arrangements for laminar and turbulent flows. All these numerical studies used variations of the finite difference

0271-2091/89/111381-14$07.00

*Received 27 October 1988*
*Revised 26 January 1989*

method for the solution of the steady-state approximation to the problem. There is only one study using a finite element method with the penalty formulation, that of Dhaubhadel *et al.*[14] who obtained the solution to a steady-state flow for a five-tube column for Reynolds numbers up to 600.

The objective of the present study is to use a finite element formulation for the numerical solution to the steady-state momentum and heat transfer problem of a tube bundle in crossflow. The technique presented in this work, suitable for high-Reynolds-numbers flows,[15-17] uses the Galerkin weighted residuals method with bilinear basis functions and a streamfunction/vorticity formulation. Numerical results for this formulation can be found in Campion-Renson and Crochet[16] for the square wall driven cavity problem at $Re = 0$ (Stokes flow), 100 and 400, and in Ikegawa[17] for a thin channel driven flow at $Re$ up to 1400. In this work a numerical solution is obtained for five tubes in a column; however, the method can be generalized to bundles of more tubes. Solutions are obtained for Reynolds numbers up to 1000. The method of solution used in this study has also been extended to the case of multiply connected regions in order to solve the problem of flexible vibrating tubes in a heat exchanger bundle.[18,19]

## 2. PROBLEM FORMULATION

The fluid velocities met in heat exchanger applications are low enough for the outside fluid to be considered incompressible. Typical heat exchanger bundles have very high length-to-diameter ratios ($l/d > 30$) so that the outside flow can be considered to be two-dimensional. Finally, only the laminar steady-state case is considered here since previous studies have shown[13,14] that the solution to the steady-state problem yields reliable results for the heat transfer and pressure drop coefficients at moderate $Re$ despite the appearance of vortices downstream.

The present study considers the two-dimensional incompressible, steady-state flow past a five-row deep in-line tube bank. The rows in the flow geometry are assumed to be of infinite extent so that the flow pattern can be considered as periodic normal to the flow direction. Therefore the computational domain is limited to the one shown in Figure 1 by the dashed lines. The five-row deep tube bank geometry is completely characterized by two dimensionless pitch ratios

$$p_1 \equiv P_1/d \quad \text{and} \quad p_2 \equiv P_2/d, \tag{1}$$

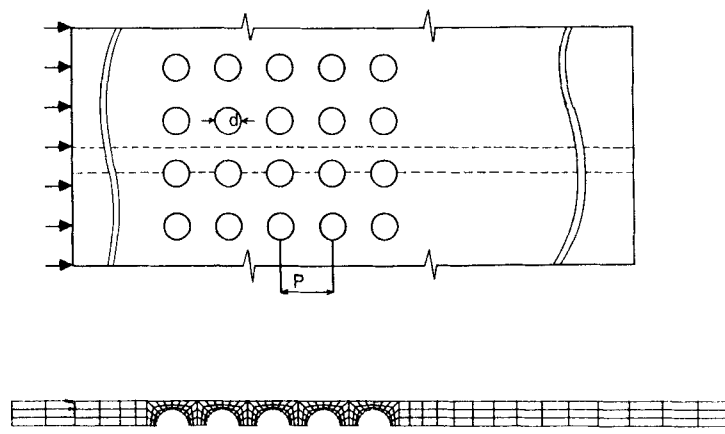


Figure 1. The five-row model and the computational domain

where $d$ is the (common) tube diameter, and $P_1$ and $P_2$ are the distances between the tube centres normal and parallel to the flow direction respectively.

The conservation equations for the flow under the previously stated assumptions are given, in a Cartesian frame of reference $x$, $y$ and in dimensionless form, as follows:

continuity

$$\frac{\partial u}{\partial x}+\frac{\partial v}{\partial y}=0; \tag{2}$$

momentum

$$u\frac{\partial u}{\partial x}+v\frac{\partial u}{\partial y}=-\frac{\partial P}{\partial x}+\frac{1}{Re}\left(\frac{\partial^2 u}{\partial x^2}+\frac{\partial^2 u}{\partial y^2}\right), \tag{3a}$$

$$u\frac{\partial v}{\partial x}+v\frac{\partial v}{\partial y}=-\frac{\partial P}{\partial y}+\frac{1}{Re}\left(\frac{\partial^2 v}{\partial x^2}+\frac{\partial^2 v}{\partial y^2}\right); \tag{3b}$$

energy

$$u\frac{\partial \theta}{\partial x}+v\frac{\partial \theta}{\partial y}=\frac{1}{RePr}\left(\frac{\partial^2 \theta}{\partial x^2}+\frac{\partial^2 \theta}{\partial y^2}\right). \tag{4}$$

In the above equations the velocities are made dimensionless by dividing with the upstream velocity $U$ and the co-ordinates by dividing with the tube diameter $d$. The dimensionless variables $\theta$ and $P$ are defined in terms of the dimensional temperature $T$ and dimensional pressure $P^*$ as

$$\theta=\frac{T-T_{in}}{T_w-T_{in}}, \tag{5a}$$

$$P=\frac{2P^*}{\rho U^2}, \tag{5b}$$

where $T_{in}$ and $T_w$ are the temperatures at the inlet and the tube wall respectively. Finally, the Reynolds number is defined by $Re \equiv Ud/\nu$.

The pressure gradient term in the momentum equations is eliminated by cross-differentiation and subtraction. The resulting equation is then given in terms of the dimensionless vorticity $\omega$ as follows:

$$u\frac{\partial \omega}{\partial x}+v\frac{\partial \omega}{\partial y}=\frac{1}{Re}\left(\frac{\partial^2 \omega}{\partial x^2}+\frac{\partial^2 \omega}{\partial y^2}\right). \tag{6}$$

The continuity equation is satisfied automatically if the velocity components are evaluated from the streamfunction $\psi$. From the definition of the vorticity, the streamfunction has to satisfy a Poisson equation:

$$\frac{\partial^2 \psi}{\partial x^2}+\frac{\partial^2 \psi}{\partial y^2}=-\omega. \tag{7}$$

Auxiliary equations are used to obtain the velocities $u$ and $v$ for the flow field and the pressure field. The two velocities may be obtained from the vorticity function by solving the following two

Poisson equations:

$$\frac{\partial^2 u}{\partial x^2}+\frac{\partial^2 u}{\partial y^2}=-\frac{\partial \omega}{\partial y}, \tag{8a}$$

$$\frac{\partial^2 v}{\partial x^2}+\frac{\partial^2 v}{\partial y^2}=\frac{\partial \omega}{\partial x}. \tag{8b}$$

In finite element post-processing calculations, it is advantageous to evaluate the velocity variables by solving the corresponding Poisson equations (equation (8) above) rather than by differentiating the streamfunction, since the latter approach leads to discontinuous profiles. For the pressure one may also obtain a Poisson equation by cross-differentiating and adding the two momentum equations. The resulting equation is

$$\frac{\partial^2 P}{\partial x^2}+\frac{\partial^2 P}{\partial y^2}=2\left(\frac{\partial u}{\partial x}\frac{\partial v}{\partial y}-\frac{\partial v}{\partial x}\frac{\partial u}{\partial y}\right). \tag{9}$$

The boundary conditions for the variables, in reference to the computational domain depicted in Figure 1, are defined in the following paragraphs. Note that the functions $f_1$ and $f_2$ used to specify the non-trivial boundary conditions for the vorticity are specified in Section 3.

At the inlet ($x = 0$) a free stream flow is assumed:

$$\psi = y, \qquad \omega = f_1(\psi, \omega), \qquad \theta = v = 0, \qquad u = 1, \qquad \frac{\partial P}{\partial x} = -Re^{-1}\frac{\partial \omega}{\partial y}. \tag{10a}$$

At the upper boundary ($y = 1$) symmetry conditions are used:

$$\psi = 1, \qquad \omega = \frac{\partial \theta}{\partial y} = \frac{\partial u}{\partial y} = v = \frac{\partial P}{\partial y} = 0. \tag{10b}$$

At the outlet ($x = L$) fully developed (in $x$) flow and temperature profiles are assumed:

$$\frac{\partial \psi}{\partial x} = \frac{\partial \omega}{\partial x} = \frac{\partial \theta}{\partial x} = \frac{\partial u}{\partial x} = \frac{\partial v}{\partial x} = 0, \qquad \frac{\partial P}{\partial x} = \omega v - Re^{-1}\frac{\partial \omega}{\partial y}. \tag{10c}$$

At the lower symmetry line ($y = 0$) the following symmetry conditions are applicable:

$$\psi = \omega = \frac{\partial \theta}{\partial y} = \frac{\partial u}{\partial y} = v = \frac{\partial P}{\partial y} = 0. \tag{10d}$$

Finally, at the surface of the tubes ($r = 0{\cdot}5$) non-slip conditions are assumed:

$$\psi = 0, \qquad \omega = f_2(\psi, \omega), \qquad \theta = 1, \qquad u = v = 0, \qquad \frac{\partial P}{\partial r} = -Re^{-1} r^{-1}\frac{\partial \omega}{\partial \phi}, \tag{10e}$$

where $r$ and $\phi$ refer to the local cylindrical co-ordinate system for each tube obtained with centre the centre of the tube.

The Galerkin weighted residuals are formed from the weak formulation of the conservation equations according to standard procedure. The same bilinear basis functions $\phi_i$ have been used in the finite element approximations and as the weighting functions in all equations. The zero normal derivative (Neumann) boundary conditions have been used to eliminate the surface integrals at the inlet, outlet and symmetry lines and to bring the resulting discrete equations to their final form.

Accordingly, the final forms of the vorticity and streamfunction equations are

$$\int_{\Omega_h^e}\left[\left(\frac{\partial\psi_h}{\partial y}\frac{\partial\omega_h}{\partial x}-\frac{\partial\psi_h}{\partial x}\frac{\partial\omega_h}{\partial y}\right)\phi_i-\frac{1}{Re}\nabla\omega_h\cdot\nabla\phi_i\right]dx=0, \tag{11}$$

$$\int_{\Omega_h^e}(\nabla\psi_h\cdot\nabla\phi_i-\omega_h\phi_i)dx=0, \tag{12}$$

where the subscript 'h' denotes the finite element approximation to the corresponding variable. The final form of the energy equation is

$$\int_{\Omega_h^e}\left[\left(u_h\frac{\partial\theta_h}{\partial x}+v_h\frac{\partial\theta_h}{\partial y}\right)\phi_i+\frac{1}{RePr}\left(\frac{\partial\theta_h}{\partial x}\frac{\partial\phi_i}{\partial x}+\frac{\partial\theta_h}{\partial y}\frac{\partial\phi_i}{\partial y}\right)\right]dx=0. \tag{13}$$

Finally, the three auxiliary equations for the two velocity components $u$ and $v$ and for the pressure $P$ are as follows:

$$\int_{\Omega_h^e}\left(\nabla u_h\cdot\nabla\phi_i-\frac{\partial\omega_h}{\partial y}\phi_i\right)dx=0, \tag{14a}$$

$$\int_{\Omega_h^e}\left(\nabla v_h\cdot\nabla\phi_i+\frac{\partial\omega_h}{\partial x}\phi_i\right)dx=0, \tag{14b}$$

$$\int_{\Omega_h^e}\left[2\left(\frac{\partial v_h}{\partial y}\frac{\partial u_h}{\partial x}-\frac{\partial v_h}{\partial x}\frac{\partial u_h}{\partial y}\right)\phi_i+\nabla P_h\cdot\nabla\phi_i\right]dx-\int_{\partial\Omega_h^e}\frac{\partial P_h}{\partial n}\phi_i\,ds=0. \tag{14c}$$

It must be pointed out that the surface integral in the last equation does not vanish and has to be evaluated using the non-homogeneous boundary conditions for the normal derivative of the pressure indicated in equations (10)—the boundary conditions for the pressure are of the Neumann type at all the surfaces. The surface integrals do not contribute in the rest of the equations because the boundary conditions for the rest of the variables are, depending on the boundary, either of the essential (Dirichlet) type or of the Neumann type corresponding to zero normal derivatives (natural boundary conditions). More details about the derivation of the equations and their transformation to discrete form may be found in Chang.[18]

## 3. NUMERICAL IMPLEMENTATION

One of the difficulties of the implementation of the streamfunction/vorticity formulation is the fact that the values of the vorticity on the solid wall and at the inlet are unknown.[15] This difficulty has been thoroughly studied in the finite difference context: see Roache[20] (Chapter III-C, pp. 140–160) for a review of the available methods to handle the missing boundary conditions. In a finite element context the extension of the finite difference techniques is straightforward; however, no information exists for their reliability and caution is required.[15] In this work, a second-order accurate boundary condition for the vorticity was found to give reliable results (the solution converges rapidly with mesh refinement).

The boundary values for the vorticity are expressed in terms of the values of the streamfunction and vorticity at the boundary, and adjacent to the boundary, nodal points. A third-order Taylor expansion of the streamfunction yields the following expression:

$$\psi_{w+1}=\psi_w+\left.\frac{\partial\psi}{\partial y}\right|_w h+\left.\tfrac{1}{2}\frac{\partial^2\psi}{\partial y^2}\right|_w h^2+\left.\tfrac{1}{6}\frac{\partial^3\psi}{\partial y^3}\right|_w h^3+O(h^4), \tag{15a}$$

where $y$ is normal to the boundary co-ordinate and $h$ is the $y$-distance between the nodal points, $w$ on the wall and $w+1$ adjacent to the wall. Furthermore, from the streamfunction equation and the definition of the vorticity we have

$$\left.\frac{\partial^2\psi}{\partial y^2}\right|_w = \omega_w \equiv -\left.\frac{\partial u}{\partial y}\right|_w. \tag{15b}$$

Substitution of the last equation into (15a) yields the following expression for the value of the streamfunction at the nodal point adjacent to the wall, $\psi_{w+1}$:

$$\psi_{w+1} = \psi_w - \tfrac{1}{2}\omega_w h^2 + \tfrac{1}{6}\frac{\partial^3\psi}{\partial y^3}h^3 + O(h^4). \tag{15c}$$

Differentiation of the vorticity function with respect to $y$ and use of the continuity equation enables the expression of the last term in equation (15c) in terms of the derivatives of vorticity. Thus the final equation for the vorticity at the wall is

$$\omega_w = \tfrac{1}{2}\omega_{w+1} - 3\frac{\psi_{w+1}-\psi_w}{h^2} \equiv f_2(\psi, \omega). \tag{16}$$

A similar equation is derived for $f_1$ and is used in the finite element method for the vorticity boundary condition ($\omega = f_1(\psi, \omega)$) at the inlet.

Because of the non-linear nature of the vorticity transport equation (6), the discretized equations, which result from the application of the Galerkin finite element method, equations (11) and (12), are non-linear and need to be solved iteratively. In the present study a simple Picard iteration technique is used for the solution of the non-linear algebraic equations. The flowchart of the iteration technique is shown in Figure 2. After solving for the streamfunction and vorticity, the two velocity components are calculated by direct solution of the linear equations obtained from the weak formulation of the Poisson equations (14a) and (14b). The energy equation is not coupled with the momentum equations and therefore is solved separately. The velocity values obtained from the solution of the Poisson equations (14a) and (14b) are put into the energy equation, which is solved for the dimensionless temperature $\theta$. Similarly, the pressure values are obtained by solving separately the Poisson equation (14c).

## 4. RESULTS AND OBSERVATIONS

### *4.1. Method validation*

The numerical scheme was tested against known analytical flow solutions. First, the Poiseuille flow was solved numerically using the above scheme. In the process of determination of the vorticity function, the convergence criterion used was a maximum fractional deviation of $10^{-5}$ for every dependent variable. The solution converged in three iterations using the Newton–Raphson method. The velocities derived from the numerical method agreed up to the sixth decimal place with the analytical solution for a mesh size involving 88 elements (8 in transverse × 11 in longitudinal direction).

Secondly, the developing flow in a channel of aspect ratio equal to 20 was calculated. For this flow a Picard iteration scheme was used. The convergence criterion for the scheme was the same as in the Poiseuille flow, and the iteration scheme for the streamfunction and vorticity equations converged in about 20 iterations for most of the Reynolds numbers examined. The numerical results were compared with the analytical solution.[21] In this case the velocity in the fully

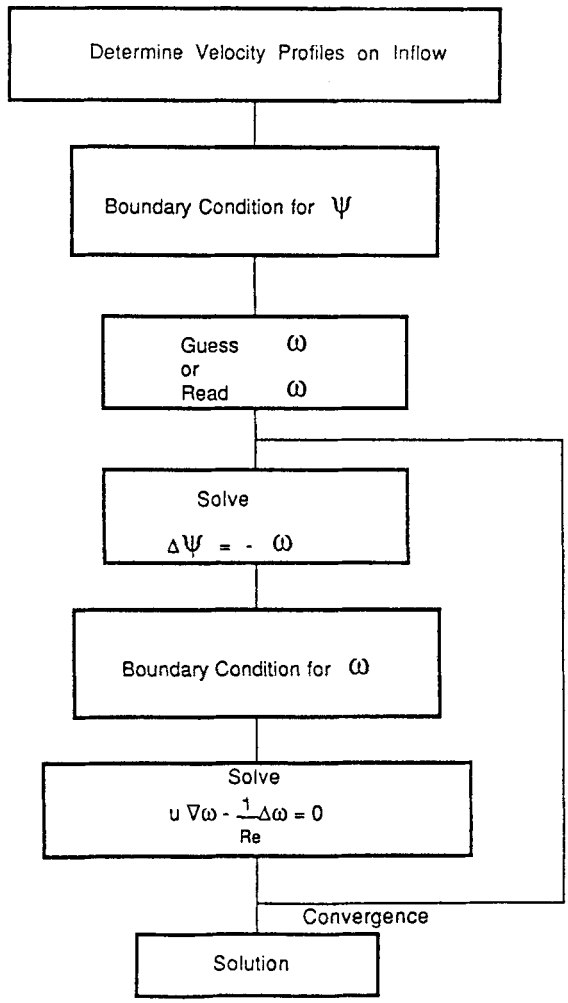


Figure 2. The procedure for Picard iteration

developed region was calculated with an accuracy of 0·001% and the development length within 1% for Reynolds numbers between 30 and 1000 for a mesh of 144 elements (8 transverse × 16 longitudinal). The two comparisons of the numerical scheme with well known results provided strong evidence of the reliability of the present method and the good resolution obtained with the mesh size used.

### *4.2. Results for the tube bundle*

The flow geometry for a five-row deep tube bundle is shown in Figure 1, where $P$ is the pitch distance and $d$ the tube diameter. Because of the geometric symmetry, the region between the broken lines was chosen as the flow domain in the numerical method. A mesh independence test was performed first for the quantities of interest. The numerical results from six different computational meshes were compared, and a mesh with 324 nodes and 240 elements resulted in less than 2% error in the tube bundle calculations. The results of the mesh test and the actual mesh

used in the calculations are shown in Figures 3 and 1 respectively. This mesh provides a dense discretization near the solid tubes. The width of the flow domain is 0·75 diameters (designed for a pitch ratio of 1·5), the entrance region is located 4·375 diameters upstream of the first tube and the exit region is 10·375 diameters in length. The inlet conditions are thus specified by actual design conditions of heat exchangers. It was also shown that even for the high-Reynolds-number cases examined, this proximity of the boundary to the first tube did not affect the derived results.

For a tube bundle of this geometry, results for eight different Reynolds numbers between 50 and 1000 were obtained. The results for the vorticity and streamfunction variables were obtained typically in 30–40 Picard iterations. The calculations for these variables required approximately 20 min CPU time on a VAX 11/785 computer. The incremental loading (parametric continuation) process was used for the calculation of the solution at successively higher Reynolds numbers.

The computed streamlines for three different Reynolds numbers are shown in Figure 4. The fluid assumed for this figure and all the subsequent ones is air ($Pr = 0{\cdot}7$). It is observed that the flow patterns are similar and that the recirculation region behind the cylinders expands with increasing Reynolds number. The same observation was made for the vorticity lines. It is also observed in Figure 4 that fluctuations in the inlet region appear for the highest Reynolds number. These fluctuations were practically eliminated when a finer mesh was used.

The velocity, pressure and temperature fields were subsequently calculated as described in Section 3. Constant vorticity lines are shown in Figure 5 and the dimensionless pressure profiles along the top symmetry line for two Reynolds numbers are shown in Figure 6. The pressure is made dimensionless by dividing with the dynamic head of the incoming flow. For this reason the results of the $Re = 540$ case lie above the results for the lower Reynolds number, a fact which is well documented from experiments.[3,22] It must be pointed out here that in Figures 4 and 5 only the general characteristics of the flow are intended to show (such as the development of recirculation zones) and not any quantitative details.

Figure 7 shows the local Nusselt number around the five tubes for $Re = 540$. It is seen that the first tube has a higher Nusselt number and that a maximum in the Nusselt number is observed.

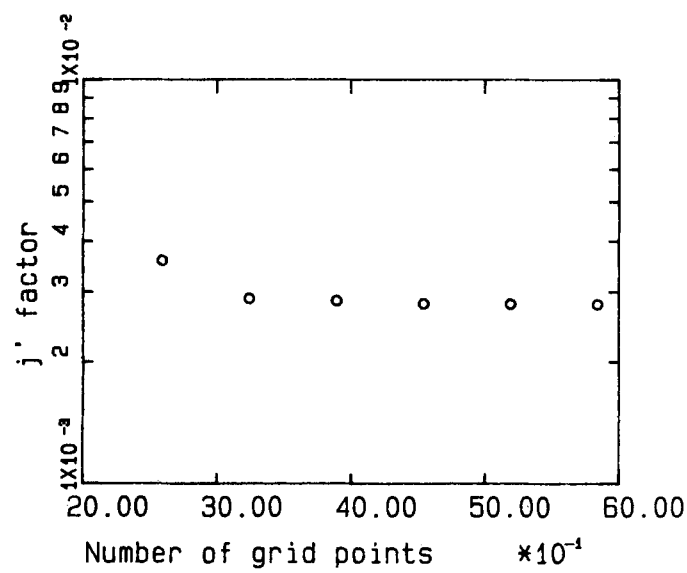


Figure 3. The results of the mesh independence test on the heat transfer coefficient

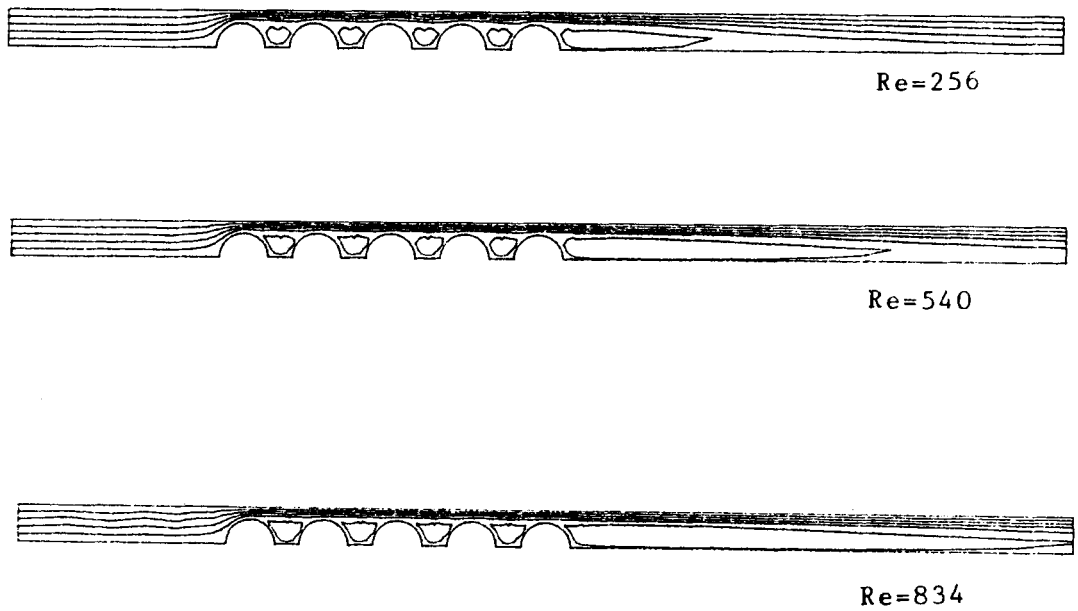


Figure 4. Flow streamlines at different Reynolds numbers for a pitch ratio of 1·5

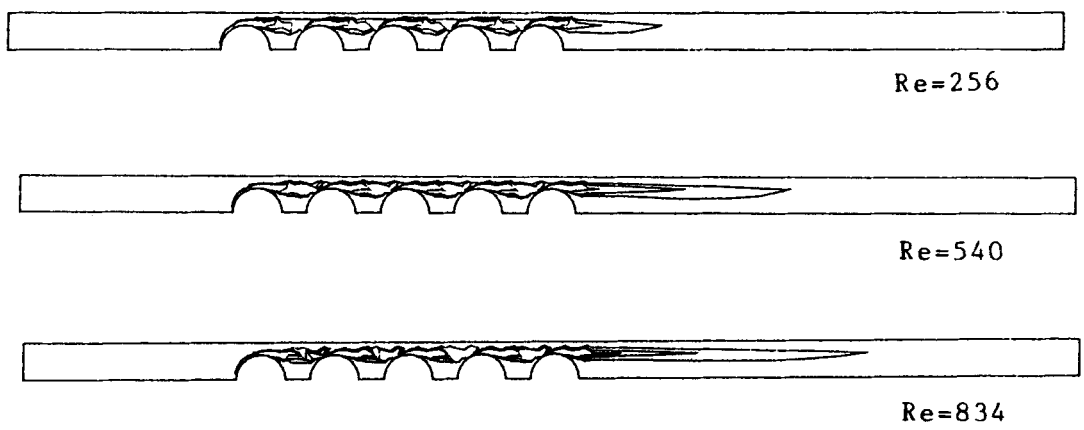


Figure 5. Constant vorticity lines at different Reynolds numbers for a pitch ratio of 1·5

This maximum is not exactly at the stagnation point of the tubes, a result also observed by others.[11,14] These results are in qualitative agreement with the analytical and experimental data for a single cylinder[7] and the numerical data for a tube bundle.[11,14]

The local Nusselt numbers were obtained from the following equation:

$$Nu \equiv \frac{\alpha d}{k} = -\frac{d}{T_{in} - T_b} \frac{\partial T}{\partial y}\bigg|_w, \tag{17}$$

where $\alpha$ is the film heat transfer coefficient, and $T_{in}$ and $T_b$ are the inlet and bulk temperatures respectively.

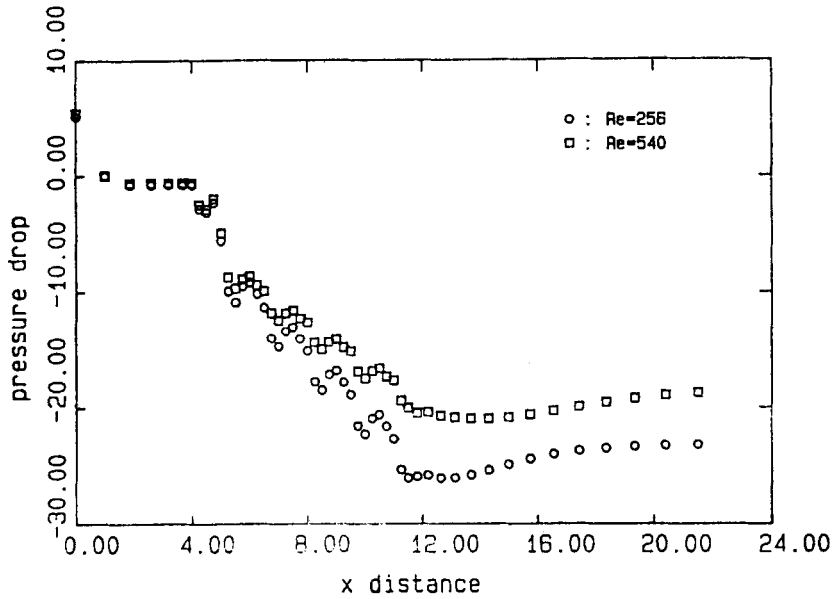


Figure 6. Computed pressure profile along the top symmetry line

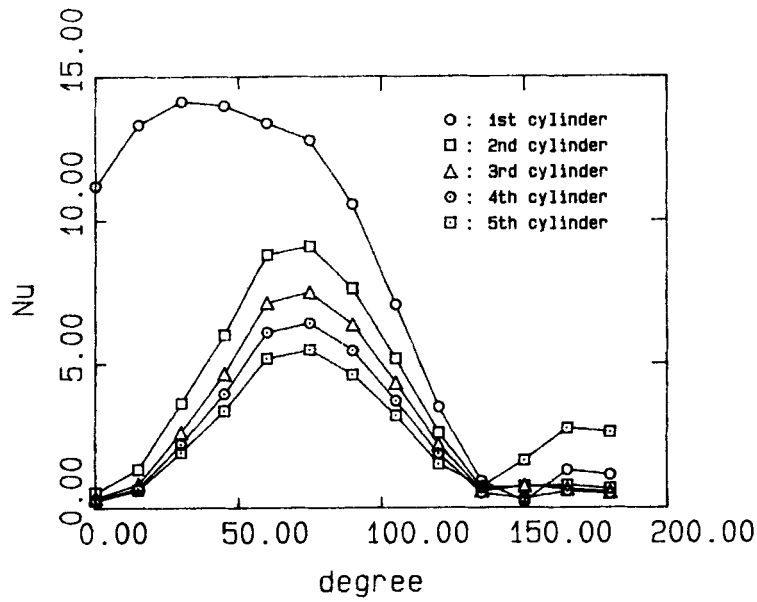


Figure 7. Local Nusselt number profiles for the five cylinders in the tube bank

The average pressure drop and Nusselt number for the tube bundle of pitch ratio 1·5 were calculated from the local results. These two quantities are of engineering interest and were determined experimentally in several projects, including those of Bergelin *et al.*,[3] Michaelides *et al.*[22] and the Engineering Standards Development Institute (ESDI) for 1973 and 1974. The results

of the present study for the average pressure drop coefficient per row are shown in Figure 8 along with other calculations and the curve obtained by Bergelin *et al.*[3] from their experimental data. It is observed that the results of the present study agree very well with the experimental curve and that there is also good agreement with the other numerical studies. The deviations of the other numerical studies from the experimental curve are attributed to the assumption of fully developed

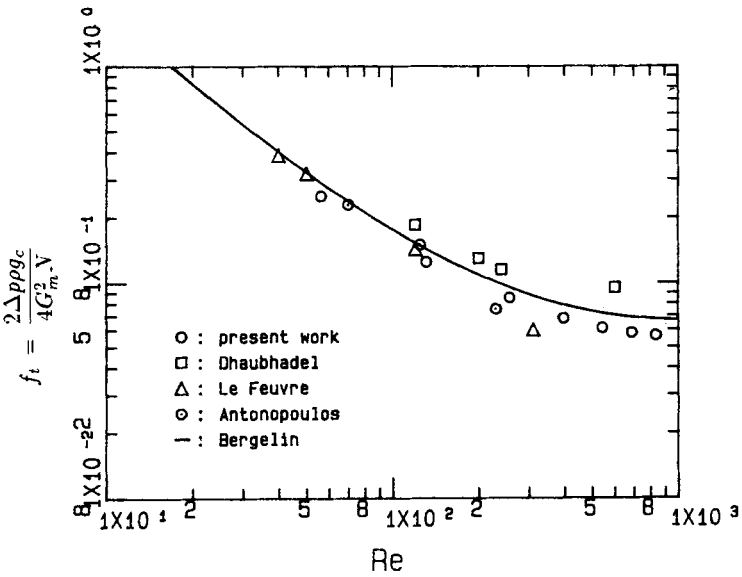


Figure 8. Average pressure drop coefficient per row of the tube bank. Comparisons with experimental data and other calculations for a pitch ratio of 1·5

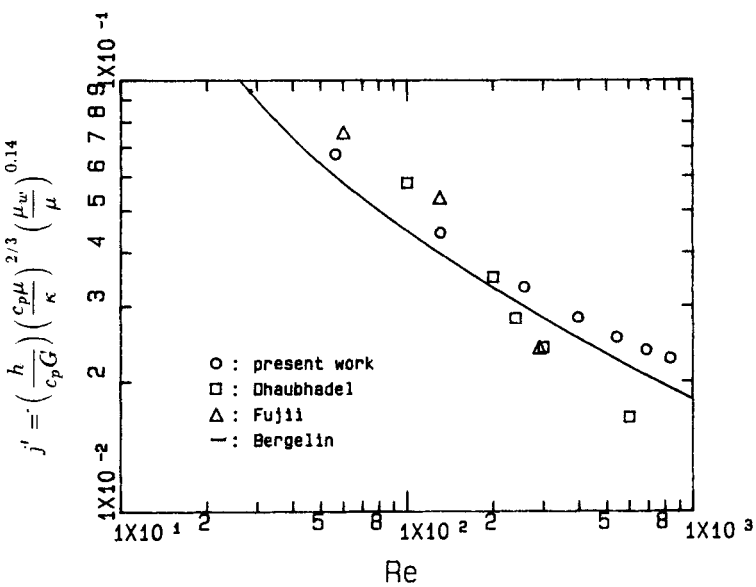


Figure 9. Modified *j*-factor based on the average heat transfer coefficient for the tube bank. Comparisons with experimental data and other calculations for a pitch ratio of 1·5

flow (negligence of entrance effects) by the other authors or to the fact that the penalty method used[14] may not be very accurate at the higher Reynolds numbers, as reported in Thomasset.[15]

Figure 9 shows the average modified $j$-factor per row of the bundle as a function of the Reynolds number. These results have been corrected for 10 rows to be in accordance with the experimental data and other numerical results. It is observed that the present data agree well with the

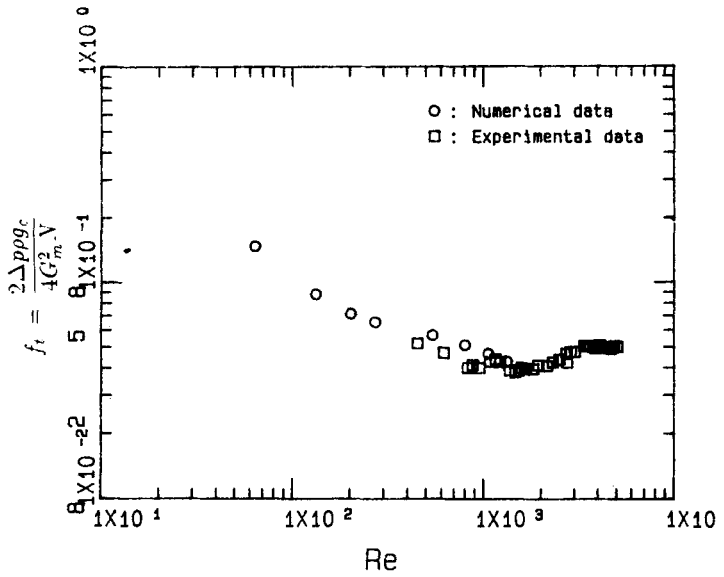


Figure 10. Calculated average pressure drop coefficient per row for a tube bank of pitch ratio 2

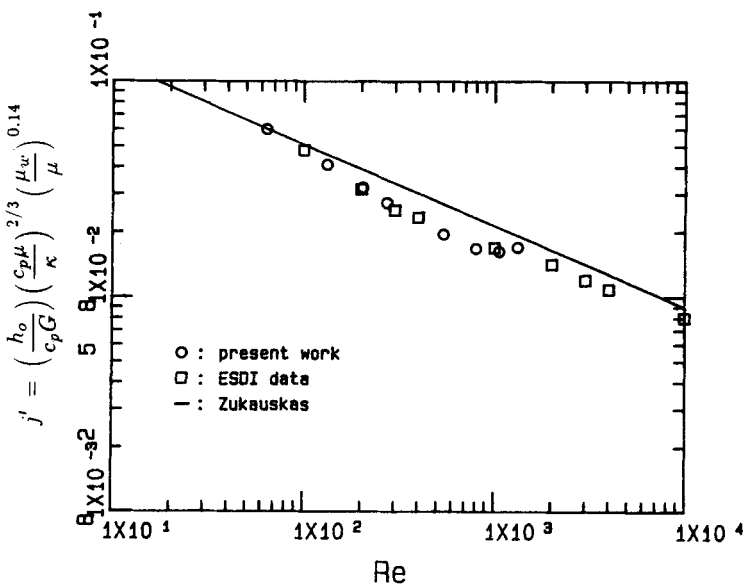


Figure 11. Modified $j$-factor based on the average heat transfer coefficient and comparisons with data for a tube bank of pitch ratio 2

experimental curve of Bergelin *et al.*[3] The small discrepancy at the higher Reynolds numbers is attributed to variations in the fluid properties with temperature, which are not accounted for in this study. It is seen, however, that the present calculations are closer to the experimental data than the other numerical predictions.

Calculations were also made using the present numerical method at a pitch ratio of 2. The results for the average pressure drop coefficient and the modified $j$-factor are shown in Figures 10 and 11 respectively. Comparisons were made with data presented by Michaelides *et al.*[22,23] and ESDI (1973) and with the correlation suggested by Zukauskas.[24] It can be observed again that the present results show good agreement with the data. The other numerical studies mentioned above do not include this geometry in their calculations.

It is well known that at Reynolds numbers above 300, instabilities in the flow develop and the flow is no longer laminar. The range $300 < Re < 3000$ belongs to the transition region for a bundle of tubes. The present study is for a laminar case and it is expected that at high Reynolds numbers it will fail in its predictions. However, comparison of calculations of the average engineering results with experimental data show that the predictions of this method for average quantities—such as the overall pressure drop or the average $j$-factor—are reliable up to Reynolds numbers of 1000. It is not recommended that the same method be used for much higher Reynolds numbers because turbulence will start dominating the flow.

## 5. CONCLUSIONS

A numerical method was developed to predict the heat transfer and pressure drop in rigid tube bundles. The conservation equations were formulated in terms of the vorticity and the streamfunction, and the Galerkin finite element technique was adopted for the solution of the steady-state laminar flow equations. A bilinear basis function was used to approximate the dependent variables, and the Picard iteration method was utilized for the solution of the resulting system of non-linear equations.

Results for square tube arrays and for pitch ratios of 1·5 and 2 were obtained. It was observed that there is good agreement with experimental data for the pressure and heat transfer coefficients up to Reynolds numbers of 1000. There is better agreement of the present study with experimental data than of the results of other numerical studies. This leads us to conclude that the solution of the problem with the finite element technique and the streamfunction/vorticity formulation yields more accurate predictions than other numerical methods.

## ACKNOWLEDGEMENTS

This study was supported in part by a grant from the DuPont Company. Computer time was freely provided by the Department of Mechanical Engineering, University of Delaware.

## REFERENCES

1. E. D. Grimison, 'Correlation and utilization of new data on flow resistance and heat transfer for gross-flow of gases over tube banks', *Trans. ASME*, **59**, 583–594 (1937).
2. O. P. Bergelin, G. A. Hull and F. W. Sullivan, 'Heat transfer and fluid friction during viscous flow across banks of tubes—III', *Trans. ASME*, **72**, 881–888 (1950).
3. O. P. Bergelin, G. A. Brown and S. C. Doberstein, 'Heat transfer and fluid friction during viscous flow across banks of tubes—IV', *Trans. ASME*, **74**, 953–960 (1952).
4. A. J. Gram, C. O. Mackey and C. S. Monroe, 'Convection heat transfer and pressure drop of air flowing across in-line tube banks', *Trans. ASME*, **80**, 25–35 (1958).
5. A. A. Zukauskas, 'Heat transfer from tubes in cross-flow', *Adv. Heat Transfer*, **8**, 93–160 (1972).

6. A. C. Mueller, 'Experimental data and correlations for tube banks', in *Low Reynolds Number Heat Exchanger Design*, Hemisphere, Washington DC, 1983.
7. A. A. Zukauskas and J. Ziugzda, *Heat Transfer of a Cylinder in Crossflow*, Hemisphere, Washington DC, 1985.
8. K. Ishihara and K. Bell, 'Friction factors for in-line tube banks at low Reynolds numbers', *AIChE Symp. Ser.*, **68**, 74–80 (1975).
9. R. F. Le Feuvre, 'Laminar and turbulent forced convection processes through in-line tube banks', *Imperial College (London) Report, Department of Mechanical Engineering HTS/74/5*, 1973.
10. B. E. Launder and T. H. Massey, 'The numerical prediction of viscous flow and heat transfer in tube banks', *J. Heat Transfer*, **100**, 565–571 (1978).
11. M. Fujii, T. Fujii and T. Nagata, 'A numerical analysis of laminar flow and heat transfer of air in an in-line tube bank', *Numer. Heat Transfer*, **7**, 89–102 (1984).
12. K. A. Antonopoulos, 'Prediction of flow and heat transfer in rod bundles', *Ph.D. Thesis*, University of London, 1979.
13. K. A. Antonopoulos, 'Heat transfer in tube banks under conditions of turbulent inclined flow', *Int. J. Heat Mass Transfer*, **28**, 1645–1656 (1985).
14. M. N. Dhaubhadel, J. N. Reddy and D. P. Telionis, 'Penalty finite element analysis of coupled fluid flow and heat transfer for in-line bundle of cylinders in cross-flow', *Int. J. Non-Linear Mech.*, **21**, 361–374 (1986).
15. F. Thomasset, *Implementation of Finite Element Methods for Navier–Stokes Equations*, Springer-Verlag, New York, 1981.
16. A. Campion-Renson and M. J. Crochet, 'On the stream function vorticity finite element solutions of Navier–Stokes equations', *Int. j. numer. methods eng.*, **8**, 1809–1818 (1978).
17. M. Ikegawa, 'A new finite-element technique for the analysis of viscous flow problems', *Int. j. numer. methods eng.*, **14**, 103–113. (1979).
18. Y. Chang, 'Heat and momentum transfer of flexible tube banks in cross flow', *Ph.D. Dissertation*, University of Delaware, 1988.
19. Y. Chang, A. N. Beris and E. E. Michaelides, 'A numerical study of heat and momentum transfer for flexible tube bundles in cross flow', *Int. J. Heat Mass Transfer*, in print, (1989).
20. P. J. Roache, *Computational Fluid Dynamics*, Hermosa, Albuquerque, NM, 1972.
21. H. L. Dryden, F. P. Murnaghan and H. Bateman, *Hydrodynamics*, Dover, New York, 1956.
22. E. E. Michaelides, Y. Chang and R. T. Bosworth, 'Heat transfer coefficients and friction factors for banks of flexible vibrating tubes in cross flow', *Proc. 8th Int. Heat Transfer Conf., Vol. 6*, 1986, pp. 2757–2762.
23. E. E. Michaelides, Y. Chang and R. T. Bosworth, 'Heat and momentum transfer processes through banks of flexible tubes in air cross-flow', *AIChE Symp. Ser. # 245*, **81**, 109–115 (1985).
24. A. A. Zukauskas, *Air Cooled Heat Exchangers*, McGraw-Hill, New York, 1980.